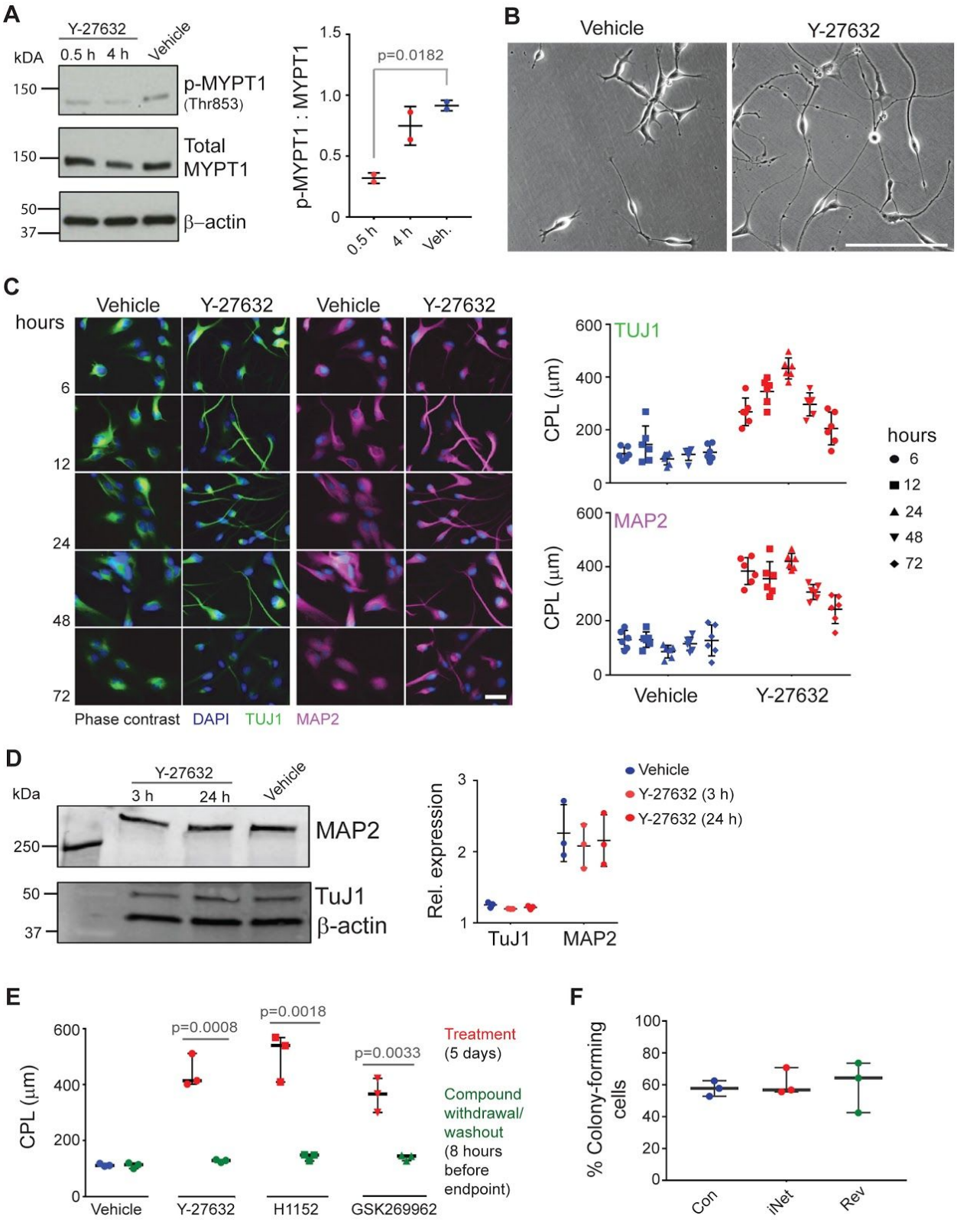

Fig. S1. Chemical ROCK inhibition reversibly induces neurite-like outgrowth in GBM1 cells. (A) Left, immunoblot detecting phosphorylated and total MYPT1 protein in LPA-stimulated GBM1

cells (1 µM, over night) followed by Y-27632 (20 µM) or vehicle (H_2O) treatments for the indicated time points. Right, the ratio of phosphorylated MYPT1 (p-MYPT1) and total MYPT1 (as determined by gel densitometry). Dots represent independent repeats. (B) Representative phase contrast images of GBM1 cells following treatment with Y-27632 (20 µM) or vehicle (H_2O) for 24 hours. Scale bar, 200 µm (C) Time course of Y-27632 (20 µM)-induced neurite-like projection outgrowth in GBM1 cells. Left, immunofluorescence images of cells and projections stained for TUJ1 and MAP2 over the indicated time course. Scale bar, 20 µm. Right, symbols are mean CPL values of three technical repeats obtained from two independent experiments (± standard deviation) comparing vehicle and Y-27632 (20 µM) treatments at the indicated time points (~200 cells analyzed per treatment experiment). (D) Left, immunoblot showing total protein levels of MAP2 and TuJ1 in GBM1 cells following the indicated treatments with Y-27632 (20 µM) or vehicle (H_2O). Right, the beta-actin control was used to normalize data yielding relative MAP2 and TuJ1 expression levels. Three independent experiments (dots, ± standard deviation) are shown. (E) Data are means of independent experiments (± standard deviation) showing TuJ1-positive CPL values in GBM1 cells after 5-day treatments with vehicle (H_2O), Y-27632 (20 µM), H1152 (10 µM), and GSK269962 (5 µM) as compared with compound withdrawal (washout) 8 hours before the experimental endpoint. (F) Clonal growth capacity of individual GBM1 cells (%) in the Con, iNet, and Rev phenotypic conditions. Data are means from three independent experiments (± standard deviation, horizontal black line: average). The p-values were determined by a two-sided Student's T-test test (equal variance).

A

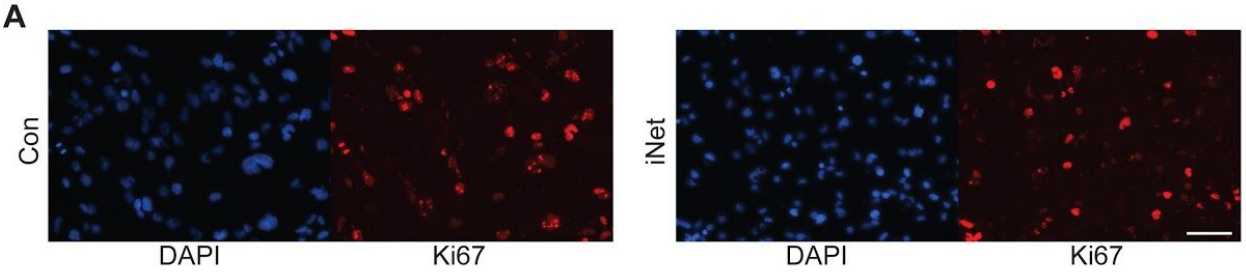

B

Category	Term	RT	Genes	Count	%	P-Value	Benjamini
KEGG_PATHWAY	Focal adhesion	RT		44	2.2	2.4E-5	6.6E-3
KEGG_PATHWAY	Hippo signaling pathway	RT		35	1.7	3.4E-5	4.7E-3
KEGG_PATHWAY	Axon guidance	RT		31	1.5	3.7E-5	3.5E-3
KEGG_PATHWAY	p53 signaling pathway	RT		20	1.0	7.5E-5	5.3E-3
KEGG_PATHWAY	Cell cycle	RT		29	1.4	1.6E-4	8.6E-3
KEGG_PATHWAY	Rap1 signaling pathway	RT		42	2.1	1.8E-4	8.2E-3
KEGG_PATHWAY	Pathways in cancer	RT		67	3.3	2.7E-4	1.1E-2
KEGG_PATHWAY	Cell adhesion molecules (CAMs)	RT		31	1.5	3.2E-4	1.1E-2
KEGG_PATHWAY	Lysosome	RT		27	1.3	6.0E-4	1.8E-2
KEGG_PATHWAY	FoxO signaling pathway	RT		29	1.4	6.0E-4	1.7E-2
KEGG_PATHWAY	TGF-beta signaling pathway	RT		21	1.0	6.4E-4	1.6E-2
KEGG_PATHWAY	HIF-1 signaling pathway	RT		23	1.1	8.3E-4	1.9E-2
KEGG_PATHWAY	HTLV-I infection	RT		46	2.3	9.7E-4	2.1E-2
KEGG_PATHWAY	Proteoglycans in cancer	RT		38	1.9	1.0E-3	2.1E-2
KEGG_PATHWAY	Central carbon metabolism in cancer	RT		16	0.8	3.5E-3	6.3E-2

C

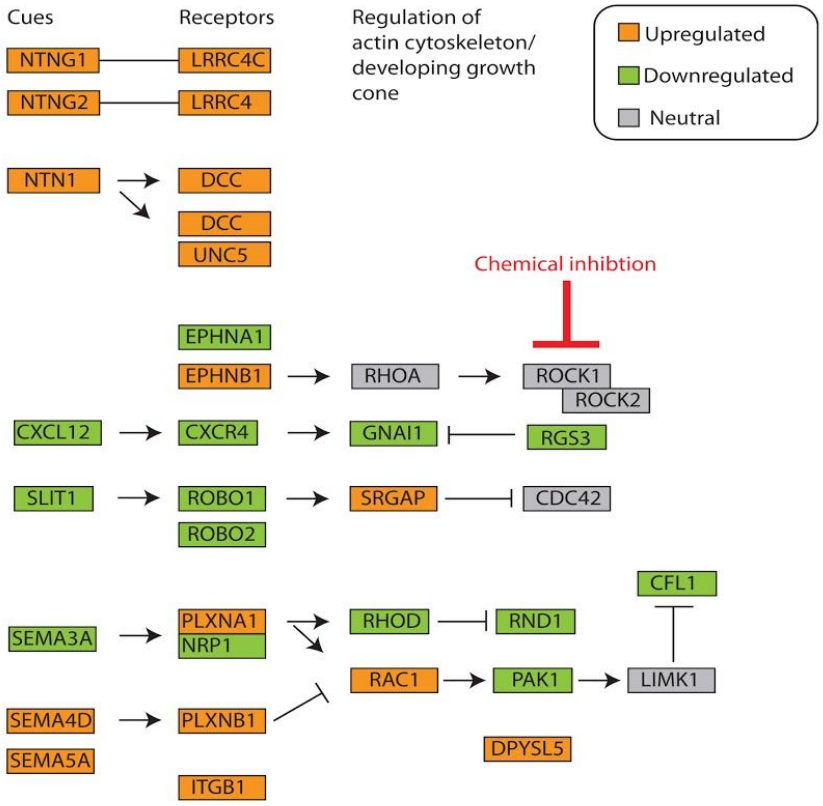

Fig. S2. GBM cells sustain proliferation and upregulate axon guidance pathways in iNet versus control conditions. (A) Representative immunofluorescence images of Ki67 staining in GBM1 cells following treatment with Y-27632 (20 µM) or vehicle (H_2O) for 24 hours. Scale bar, 50 µm. (B) DAVID functional annotation suggests iNet-specific enrichment of axonal guidance- and actin cytoskeleton-regulating genes. A list of kyoto encyclopedia of genes and genomes (KEGG; (Kanehisa and Goto 2000)) pathways that were differentially regulated ($p<0.005$) in the iNet compared with the Rev (RNA expression) profile of GBM1 cells is provided. (C) Scheme displaying the 31 genes of the KEGG axon guidance pathway that were significantly enriched in the iNet profile.

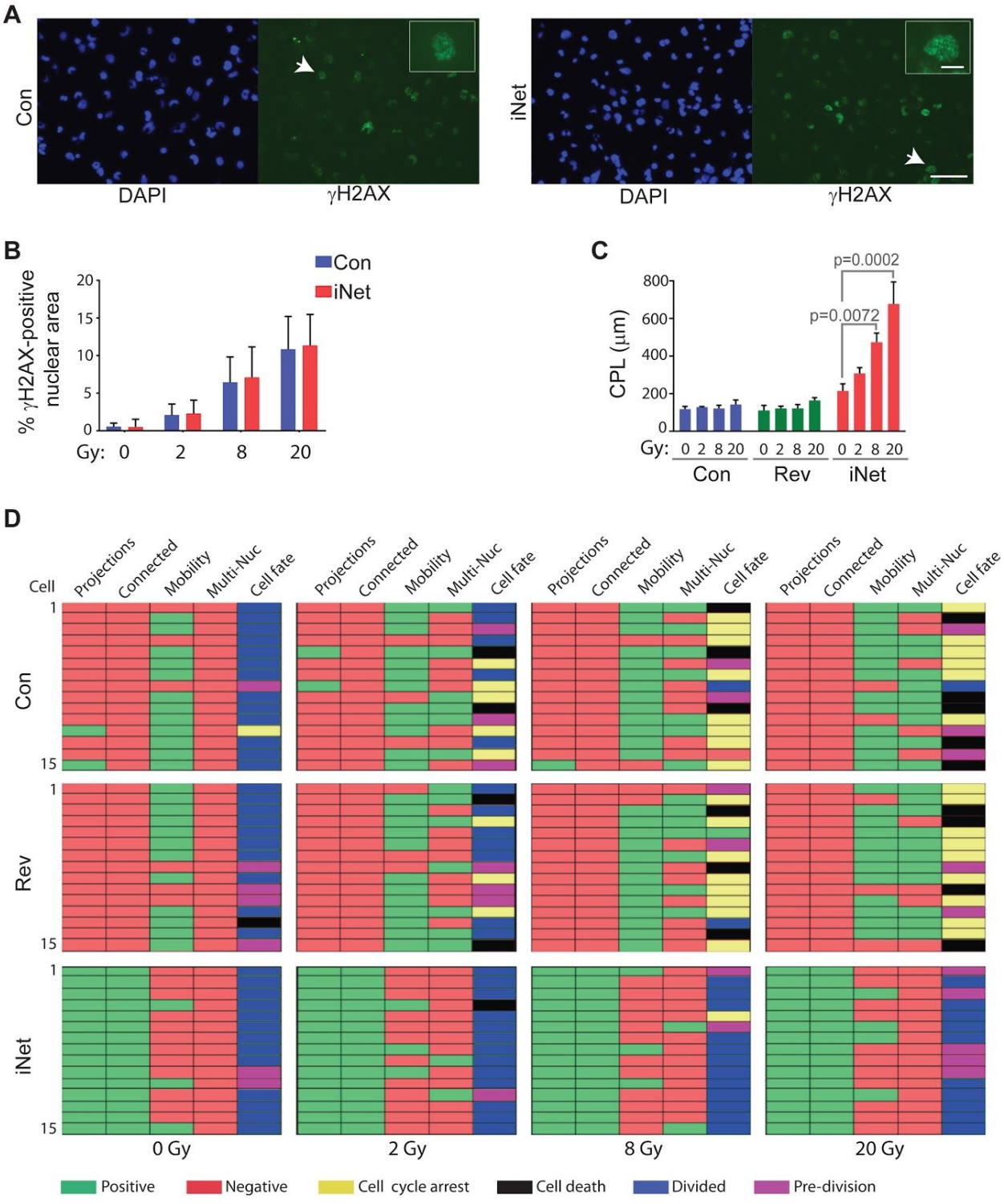

Fig. S3. GBM1 iNET cells exhibit increased cell projection outgrowth and survival upon radiation treatment. (A) Representative immunofluorescence images of DAPI (blue) and γH2AX (green) staining following 8 Gy radiation treatment in Con or iNet conditions. Arrowhead depicts damaged nuclei and punctate γH2AX foci shown in (higher zoom) inlay panels. Scale bars, 50

µm and 5 µm (inlay). (B) Quantification of γH2AX-stained nuclear area in GBM1 cells under Con and iNet phenotypic conditions 2 hours after 0, 2, 8, and 20 Gy radiation treatments. Data are means of three independent experiments (bars: mean + standard deviation) using 5 different imaging fields (>200 cells) per repeat. (C) Data are mean CPL values of three independent experiments (bars: mean + standard deviation) per Con, iNet, and Rev conditions 5 days after 0, 2, 8, and 20 Gy radiation treatments. The p-values were determined by 1-Way ANOVA. (D) Cell behaviour analysis depicting the presence (green bars) or absence (red bars) of the indicated cell morphologies (elongated projections, connections with other cells, cell mobility, multi-nucleation), and cell fates (color code: cell cycle arrest, yellow; cell division, blue; pre-division cell state, purple; cell death, black) as assessed by real time imaging for 15 cells randomly-chosen from Con, Rev, and iNet GBM1 cultures treated with the indicated radiation doses. Data indicate that most iNet cells were connected via cell projections and displayed a low motility phenotype. Taking the total of 45 analyzed cells in all radiation treatments into account, both cell cycle arrest and cell death were reduced by ~90%, and multinucleation by ~80% in iNet cells compared to their Con and Rev counterparts. Thirty-five irradiated iNet cells underwent mitosis, whereas only 7 and 8 Con and Rev cells divided, respectively.

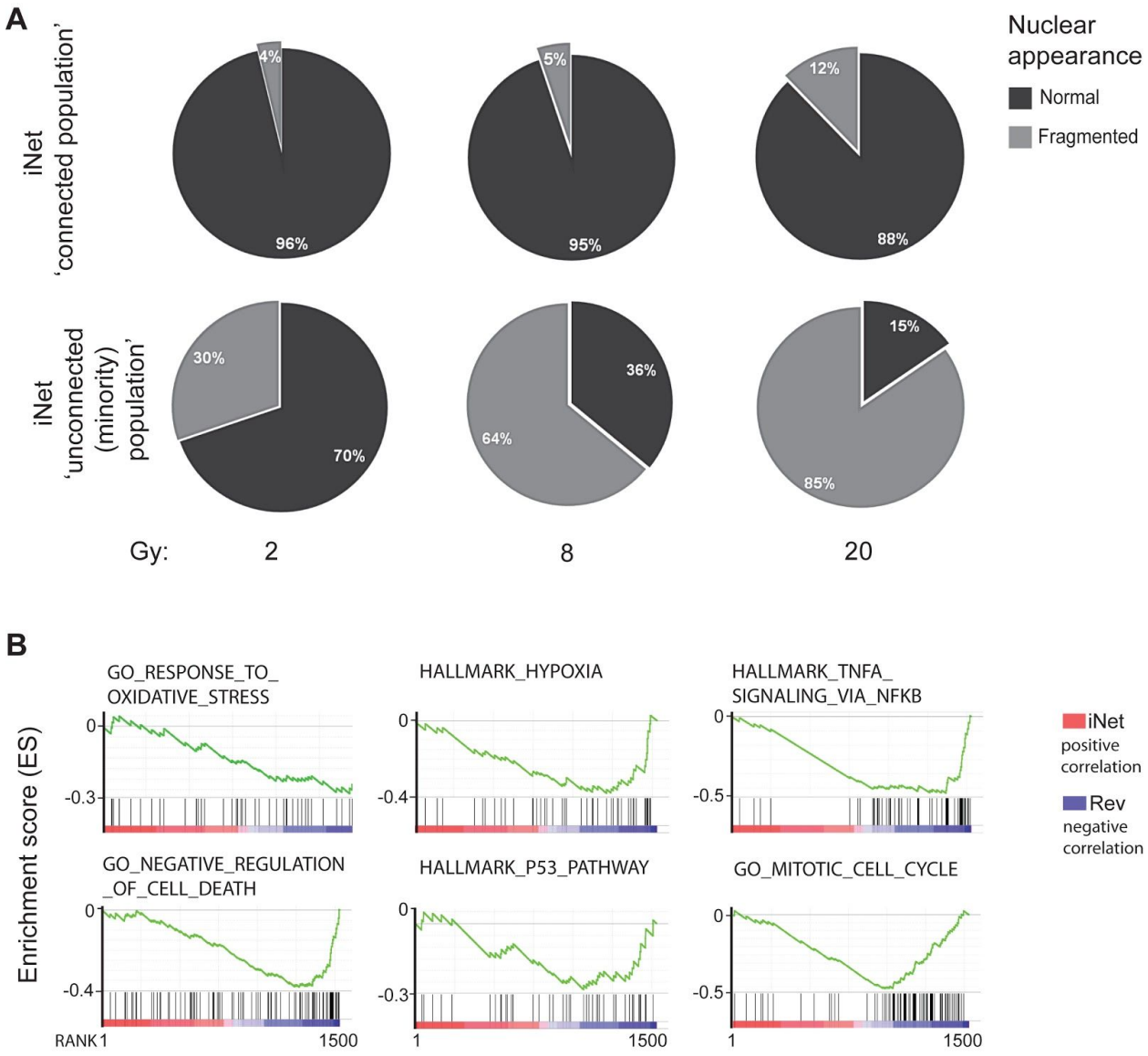

Fig. S4. Nuclear damage in the iNet phenotypic conditions was associated with the non-connected cellular subpopulation of total iNet cells. (A) GBM1 cells in iNet conditions were exposed to the indicated radiation doses and pie charts depict the percentages of fragmented nuclei 5 days post radiation treatment. (B) GSEA plots of ranked gene expression (FDR <5%) comparing transcriptional iNet and Rev profiles upon 20 Gy radiation and their positive (red) and negative (blue) correlations for the indicated gene sets. Enrichment scores are shown as green lines, and the horizontal black bars indicate the position of associated genes for each gene set. Plots suggest that the iNet RNA expression was positively-correlated with the indicated Gene Ontology Consortium (GO, Ashburner et al. 2000; The Gene Ontology Consortium 2017) and HALLMARK pathways (Liberzon et al. 2015) as compared with the negatively-correlated Rev phenotype profile in GBM1 cells.

SUPPLEMENTAL MOVIES

Movie 1. GBM1 cell model, vehicle (H_2O) treatment, time lapse period: 24 hours.

Movie 2. GBM1 cell model, Y-27632 (20 µM) treatment, time lapse period: 24 hours.

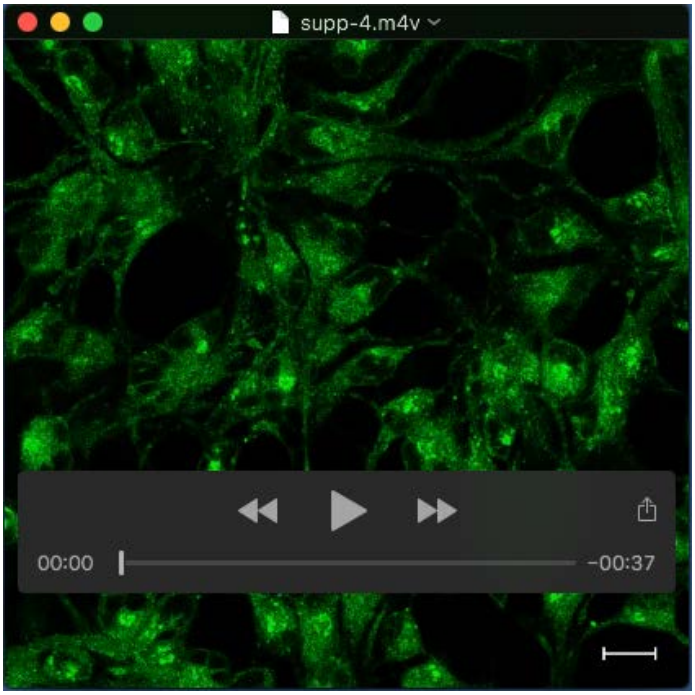

Movie 3. GBM1 cell model, Con phenotype, Mitotracker labelling (red), time lapse period: 30 minutes. Scale bar, 20 µm.

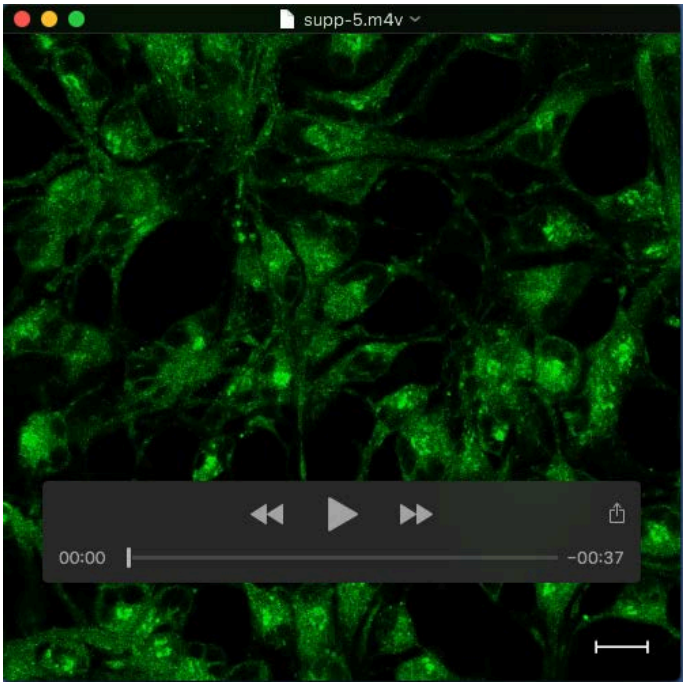

Movie 4. GBM1 cell model, iNet phenotype, Mitotracker labelling (red), time lapse period: 30 minutes. Scale bar, 20 µm.

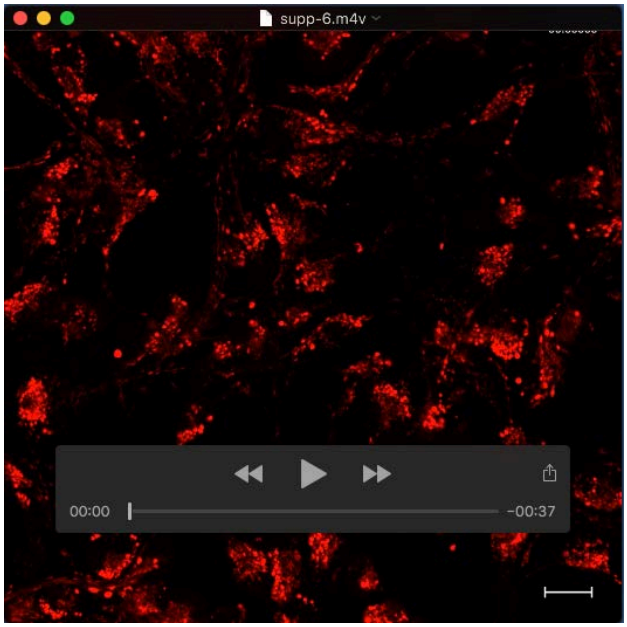

Movie 5. GBM1 cell model, Con phenotype, Lysotracker labelling (green), time lapse period: 30 minutes. Scale bar, 20 µm.

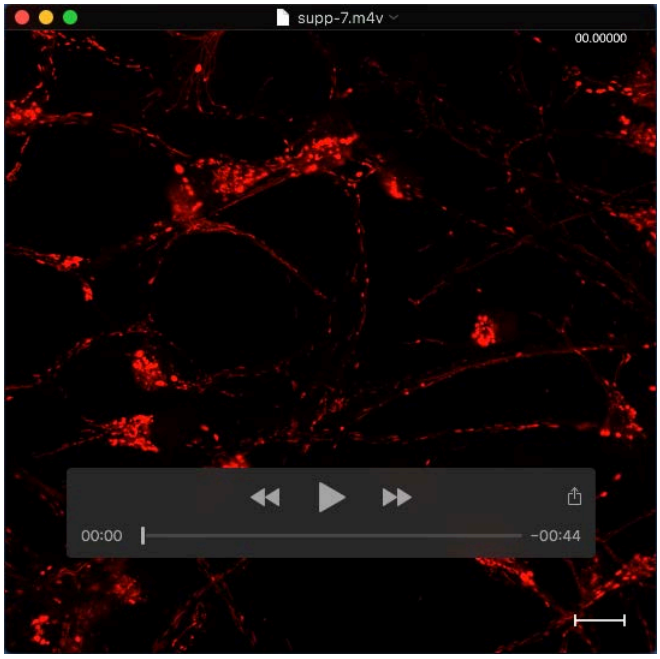

Movie 6. GBM1 cell model, iNet phenotype, Lysotracker labelling (green), time lapse period: 30 minutes. Scale bar, 20 µm.